

# Use of Multiple-Tube Phantom: A Method to Globally Correct Native T1 Relaxation Time Inhomogeneity in Dedicated Molecular Magnetic Resonance Breast Coil

Pradeep Singh Negi<sup>1,2</sup>, Shashi Bhushan Mehta<sup>1,2</sup>, Amarnath Jena<sup>1,2</sup>

<sup>1</sup>Department of Molecular Imaging and Nuclear Medicine, PET SUITE, Indraprastha Apollo Hospitals, New Delhi, <sup>2</sup>Department of Physics, Vivekananda Global University, Jaipur, Rajasthan, India

## Abstract

**Background:** Native T1 relaxation time ( $T_{10}$ ) presents an important prerequisite to reliably quantify pharmacokinetic parameter like  $K^{\text{trans}}$  (volume transfer constant). Native T1 value can be varied because of the inhomogeneity in the breast coil, thus influencing the  $K^{\text{trans}}$  measurement. **Purpose:** The current study aims to design and use a phantom with multiple tubes for both breast cuffs to assess native T1 inhomogeneity across the dedicated molecular magnetic resonance (mMR) breast coil and adopt corrective method to spatially normalize T1 values to improve homogeneity. **Materials and Methods:** Two phantoms with multiple tubes (19 tubes) specially designed and filled with contrast medium with known T1 value were placed in each mMR breast coil cuff. Native T1 at various spatial locations was calculated applying dual flip angle sequence. Correction factors were derived at various spatial locations as a function of deviation of the native T1 value from phantom and applied to correct the native T1 relaxation time. **Results:** A statistically significant difference between native T1 values of the right and left anterior ( $P = 0.0095$ ), middle ( $P = 0.0081$ ), and posterior ( $P = 0.0004$ ) parts of the breast coil. No significant difference was seen in the corrected T1 values between anterior ( $P = 0.402$ ), middle ( $P = 0.305$ ), and posterior ( $P = 0.349$ ) aspects of both sides of the breast coil. **Conclusion:** Inhomogeneity in the native T1 value exists in dedicated mMR breast coil, and significant improvement can be achieved using specially designed external phantom with multiple tubes.

**Keywords:** Dynamic contrast-enhanced magnetic resonance imaging, inhomogeneity, multiple-tube phantom, native T1

Received on: 14-01-2020

Review completed on: 29-01-2021

Accepted on: 09-02-2021

Published on: 05-05-2021

## INTRODUCTION

Breast cancer is currently the most commonly diagnosed cancer in women and accounts for approximately 22.9% of all cancers worldwide.<sup>[1]</sup> Dynamic contrast-enhanced (DCE) magnetic resonance imaging (MRI) has emerged as a novel modality for early breast cancer evaluation and surveillance and to assess response to various treatment options. However, the characterization of a lesion detected in MRI still remains a challenge with specificities in clinical studies reported between 20% and 100%.<sup>[2-8]</sup>

Fast dynamic MRI through pharmacokinetic (PK) modeling indirectly measures neovascularity and is related to computation of volume transfer constant ( $K^{\text{trans}}$ ), rate constant ( $k_{ep}$ ), and extravascular extracellular volume fraction ( $v_e$ ).<sup>[9-12]</sup> With PK modeling, the alterations in contrast agent concentration in

tissue are translated to changes in signal intensity denoted by the alterations in the relaxation time of native T1 value. The accuracy of native T1 calculation is thus pivotal for PK parameter estimation but itself is known to be influenced by a number of factors such as B1 inhomogeneity, optimization of flip angle, RF inhomogeneity, nonlinear RF amplifier, and distortions in slice profile. B1 inhomogeneity in variable flip angle (VFA) measurement also leads to substantial (around 52%) deviation in the T1 value of fat.<sup>[13,14]</sup> In the event of

**Address for correspondence:** Mr. Pradeep Singh Negi,  
Department of Molecular Imaging and Nuclear Medicine, PET SUITE,  
Indraprastha Apollo Hospitals, Sarita Vihar, Delhi–Mathura Road,  
New Delhi - 110 076, India.  
E-mail: pradeepnegi1979@gmail.com

This is an open access journal, and articles are distributed under the terms of the Creative Commons Attribution-NonCommercial-ShareAlike 4.0 License, which allows others to remix, tweak, and build upon the work non-commercially, as long as appropriate credit is given and the new creations are licensed under the identical terms.

**For reprints contact:** WKHLRPMedknow\_reprints@wolterskluwer.com

**How to cite this article:** Negi PS, Mehta SB, Jena A. Use of multiple-tube phantom: A method to globally correct native T1 relaxation time inhomogeneity in dedicated molecular magnetic resonance breast coil. J Med Phys 2021;46:41-6.

### Access this article online

#### Quick Response Code:



Website:  
www.jmp.org.in

DOI:  
10.4103/jmp.JMP\_2\_20

tumors, a 1% increase in T10 could result in a 1% decrease in  $K^{\text{trans}}$  because the measured  $K^{\text{trans}}$  value is very sensitive to the  $T1_0$  value.<sup>[15]</sup>

Among the various methods employed to measure native T1, VFA and dual flip angle (DFA) are the most common ones used to measure native T1 for PK calculations. The VFA technique uses several short-repetitive-time radiofrequency acquisitions with different flip angles. The inhomogeneity observed across the breasts affects the flip angle at different locations finally leading to substantial variations in the value of T1.<sup>[2,13,16-19]</sup>

Several studies have reported multiple methods to homogenize the magnetic field by adapting specialized coils, shimming-based technologies, or correction of B1 map to address the inhomogeneities. Yuan *et al.* in their study used DFA and multiple flip angle for the assessment of PK parameters and reported DFA 2° and 15° to return comparable results.<sup>[11]</sup> Tsai *et al.* too reported employment of VFA (with or without computed B1 correction) to correct native T1 values on observation of asymmetry of the average flip angle of 119% (left breast) and 97% (right breast) with an overall difference of 22% between the two sides.<sup>[16]</sup>

Further attempts were also made to adopt methods to normalize native T1 values directly instead of limiting various influential factors to improve T1 measurements, wherein a prefilled phantom with known T1 value was placed within the field of view (FOV) of breast coil cuffs. However, such a method to correct inhomogeneity has inherent limitations to normalize global inhomogeneity (bilateral breast coil cuff). Thus, it is prudent to hypothesize that correction factor for each spatial location could enhance global homogeneity. In the said context, the proposed study attempts to homogenize the physical space of the breast coil cuff by applying a number of correction factors derived for each spatial location using multiple-tube phantom placed in each coil cuff (as external standards). Thus, the current work was designed first to note the pattern of T1 inhomogeneity that existed in our experiment and second to see the influence of the spatial correction at multiple locations to achieve global homogeneity.

## MATERIALS AND METHODS

In the present study, we used a prototype-designed 19-tube phantom for each side of breast coil cuff, placed in the field of breast coil to measure the deviation of T1 value at each spatial location. This corrects the inhomogeneity present in the calculated T1 value at various planes in the space of the breast coil.

### Phantom creation

Two 19-tube phantoms were created for both cuffs of the dedicated receiving molecular magnetic resonance (mMR) breast coil filled with known contrast (3.75 g  $\text{NiSO}_4 \times 6 \text{H}_2\text{O}$  + 5 g NaCl per 1000 g  $\text{H}_2\text{O}$  distilled water). Each tube of phantom measured 16 cm in length and 4 cm diameter and fixed at 2 cm gap. The phantoms were placed such that each cuff space was

maximally covered by the tubes. Prototype phantom design has been reported in many formats: circle and square with 5, 16, 19, and 20 tubes. As breast coil cuffs are circular, 20 and 16 tubes in a square format did not fit well in breast coil with the medial and lateral aspect of the cuff remained unfilled with tubes and hence were not used. Thus, 19-tube phantom circular format with tubes arranged in 3, 4, 5, 4, and 3 rows was used in this study and was found to be best fitted in breast coil [Figure 1].

### Data acquisition and imaging protocol

Phantoms were examined using simultaneous positron emission tomography/MRI biograph mMR (Siemens, Erlangen, Germany) in the four-channel mMR breast coil. The manually designed phantom placed in the coil cuffs was placed at the isocenter of the magnet. MRI acquisition was performed in a fix mode. After localization obtained in three orientations, 2° flip angle proton density and 15° flip angle nonfat-suppressed T1-weighted three-dimensional (3D) images (volume-interpolated body examination [VIBE]) sequence: echo time 1.8 ms, repetition time 5.2 ms, FOV 360 mm, slices 36, accusation time 20.7s, resolution 256 × 256, and voxel size (4.4 mm × 1.4 mm × 4.0 mm) were used for native T1 calculation, acquired in coronal planes covering both breast coil cuffs completely.<sup>[10,20]</sup>

### Region of interest creation and data compilation

The region of interest (ROI) on corresponding images to derive image intensity in 2° and 15° flip angle images was used in T1 calculation. ROI was manually drawn over each tube on both sides of the breast coil phantom on the 15° flip angle images (number of pixels and area: 44, 0.22<sup>2</sup>/cm) and copy pasted on 2° flip angle images in all 36 slices. Corresponding ROI intensity values of 2° and 15° flip angle images of all the ROIs were manually entered in an Excel sheet and the native T1 values were calculated. Out of 36 slices that were acquired in 3D VIBE sequence, one slice at each terminus was excluded. Total 646 ROIs (19 ROIs in each slice × 34 slices) in each coil cuff was used for data analysis.

### Image processing

For evaluation of native T1 in a phantom study, the nonfat-suppressed T1-weighted precontrast 2° and 15° flip angle VIBE series were manually evaluated separately for native T1 calculation. The native T1 was calculated with the help of equations 1 and 2 manually in an Excel sheet.<sup>[20,21]</sup>

$$\text{Equation 1} \quad T_{10}^{-1} = \frac{1}{TR} \ln \left[ \frac{S_R \text{Sin}\alpha 2 \text{Cos}\alpha 1 - \text{Sin}\alpha 1 \text{Cos}\alpha 2}{S_R \text{Sin}\alpha 2 - \text{Sin}\alpha 1} \right]$$

$$\text{Equation 2} \quad S_R = \frac{S_{\alpha 1}}{S_{\alpha 2}}$$

$S_{\alpha 1}$  = Intensity value at  $\alpha 1$  (2° flip angle),  $S_{\alpha 2}$  = Intensity value at  $\alpha 2$  (15° flip angle), TR = Repetition time, and ln = Natural Log

### Inhomogeneity in a phantom study

The inhomogeneity of the breast coil was noted by comparing the deviation in T1 value of ROI at each location

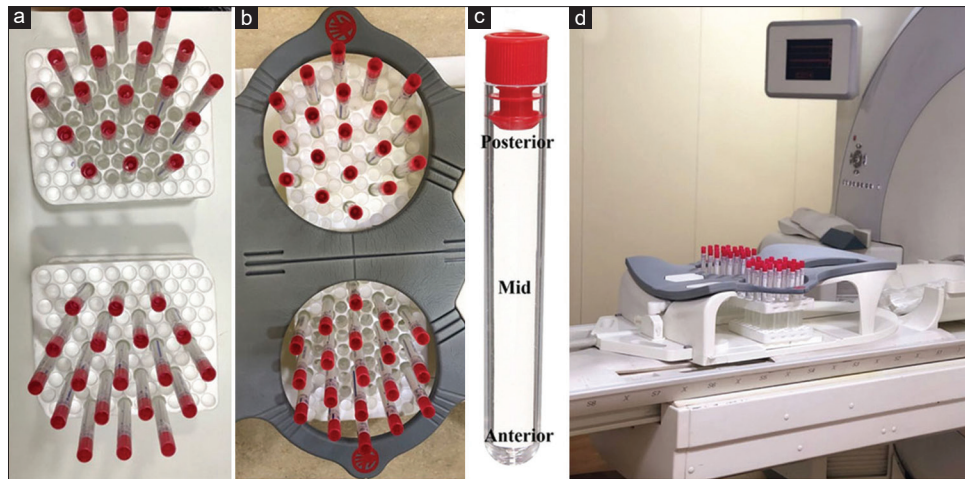


**Figure 1:** (a) Nineteen tubes in each phantom (right and left) filled with known contrast ( $280 \pm 10$  ms) were arranged as 3, 4, 5, 4, and 3 in the first, second, third, fourth, and fifth rows, respectively; (b) phantoms placed in breast coil. (c) The anterior, middle, and posterior parts of the coil and phantom tube and (d) placement of 19-tube phantom with contrast in breast coil in Siemens Biograph molecular magnetic resonance system

in 19-tube phantoms from vendor-provided known native T1 ( $280 \pm 10$  ms) value of the phantom. Variation in T1 values was documented for each side of the breast coil and from lateral to medial, anterior to posterior, and head to feet on each side.

### Statistical analysis

Two-tailed *t*-test was performed between corrected and noncorrected native T1 values on every spatial location of the breast coil at each side. The statistical analysis was performed using SPSS software package (version 19.0; SPSS for windows, 2009), IBM, Chicago, U.S.A.

## RESULTS

A significant difference in native T1 values was observed for ROIs from the anterior to the posterior part of the breast coil (anterior right  $234 \pm 19$ , anterior left  $257 \pm 32$  [ $P = 0.0095$ ], mid right  $275 \pm 23$ , mid left  $297 \pm 24$  [ $P = 0.0081$ ], posterior right  $218 \pm 8$ , and posterior left  $240 \pm 22$  [ $P = 0.0004$ ]). We also noted that there was a significant difference in T1 values of both sides of coil cuffs ( $P = 0.0004$ ) [Table 1].

### Correction factor in phantom

Inhomogeneity in T1 distribution was noted on both sides of the breast coil, and each part in the phantom study was corrected with the help of correction factor for each ROI location using the following equation (3,4).

$$\text{Equation 3} \quad Cf = \frac{Kc - t1}{Kc}$$

$t1$  = Measured T1 value phantom,  $Kc$  = T1 Value of known contrast medium ( $280 \pm 10$  ms), and  $Cf$  = Correction factor.

The formula was used for correcting the T1 value

$$\text{Equation 4} \quad Ct1 = nCt1 + (nCt1 \times Cf)$$

$Ct1$  = Corrected T1,  $Cf$  = Correction factor, and  $nCt1$  = Noncorrected T1

### Phantom T1 value after correction

Difference in native T1 values within individual parts of the breast coil was noted with dispersion of values in the right breast coil from 187 to 282 (anterior part), 223–314 (middle part), and 207–283 (posterior part) and dispersed T1 values of 212–360; 253–345, and 195–229 in the corresponding parts of the contralateral left breast coil. The T1 value at center area of the coil is more homogeneous as compared with peripheral region and matched with true T1 phantom value provided by the vendor ( $280 \pm 10$  ms).

The mean T1 value for the right breast coil was found to be  $218 \pm 8$  (posterior part),  $234 \pm 19$  (anterior part), and  $275 \pm 23$  (middle part) and was changed to  $270 \pm 4$ ,  $272 \pm 7$ , and  $278 \pm 2$ , respectively, in the corresponding part of the breast coil after applying correction factor. Similarly, the mean T1 value for the left breast coil that was found to be  $240 \pm 22$  (posterior part),  $257 \pm 32$  (anterior part), and  $297 \pm 24$  (middle part) and was changed to  $272 \pm 6$ ,  $274 \pm 6$ , and  $276 \pm 4$ , respectively, after applying correction factor [Figure 2 and Table 1]. No significant difference was observed in the corrected T1 values in the anterior ( $P = 0.402$ ), posterior ( $P = 0.349$ ), and middle parts ( $P = 0.305$ ) of the right and left breast coil. There was no significant difference in corrected T1 values of both sides of coil cuffs ( $P = 0.438$ ).

## DISCUSSION

Reliable estimation of native T1 of tissue under investigation is a prerequisite to accurate measurement of PK parameters. This assumes importance because of increasing application of PK parameters to assess the neoangiogenesis property of cancer and in particular its application in breast cancer diagnosis.<sup>[2,13,14,16-18]</sup>

Nonuniformity of the radiofrequency transmit field (B1+) observed across the breast coils reported to cause variation in the flip angle which results in a 61% T1<sub>0</sub> difference in fat and a 41.5% difference in parenchyma between the two breasts.<sup>[2]</sup>

**Table 1: The distribution of native T1 values before and after correction in different spatial location in breast coil at both sides**

Tube number	Anterior part of coil						Middle part of coil						Posterior part of coil											
	Precorrection			Postcorrection			Precorrection			Postcorrection			Precorrection			Postcorrection								
	Rt. T1	Lt. T1	Rt. CT1	Lt. CT1	Rt. T1	Lt. T1	Rt. CT1	Lt. CT1	Rt. T1	Lt. T1	Rt. CT1	Lt. CT1	Rt. T1	Lt. T1	Rt. CT1	Lt. CT1	Rt. T1	Lt. T1	Rt. CT1	Lt. CT1				
1	220.81	229.05	267.49	270.73	252.61	289.93	277.32	279.65	211.43	257.50	275.21	278.19	220.81	229.05	267.49	270.73	252.61	289.93	277.32	279.65	211.43	257.50	275.21	278.19
2	215.39	223.39	265.09	268.56	240.70	272.01	274.48	279.77	217.67	241.97	270.12	274.83	215.39	223.39	265.09	268.56	240.70	272.01	274.48	279.77	217.67	241.97	270.12	274.83
3	187.87	212.29	249.68	263.62	223.62	253.98	268.65	277.58	222.25	218.44	268.09	266.47	187.87	212.29	249.68	263.62	223.62	253.98	268.65	277.58	222.25	218.44	268.09	266.47
4	244.37	254.81	277.65	277.73	293.26	324.07	279.37	273.06	226.65	283.37	275.84	279.96	244.37	254.81	277.65	277.73	293.26	324.07	279.37	273.06	226.65	283.37	275.84	279.96
5	222.41	255.12	277.28	277.79	288.63	309.78	279.73	276.83	229.51	257.09	270.89	278.13	222.41	255.12	277.28	277.79	288.63	309.78	279.73	276.83	229.51	257.09	270.89	278.13
6	233.35	236.49	272.23	273.24	267.78	288.94	279.47	279.71	222.61	244.74	272.24	275.56	233.35	236.49	272.23	273.24	267.78	288.94	279.47	279.71	222.61	244.74	272.24	275.56
7	217.25	230.70	265.94	271.32	251.62	274.77	277.12	279.90	226.20	222.06	269.66	268.01	217.25	230.70	265.94	271.32	251.62	274.77	277.12	279.90	226.20	222.06	269.66	268.01
8	282.03	280.58	279.99	280.00	314.20	345.21	275.82	264.81	207.71	279.55	278.33	280.00	282.03	280.58	279.99	280.00	314.20	345.21	275.82	264.81	207.71	279.55	278.33	280.00
9	233.75	280.87	279.06	280.00	297.90	331.37	278.86	270.58	225.43	259.46	279.37	278.49	233.75	280.87	279.06	280.00	297.90	331.37	278.86	270.58	225.43	259.46	279.37	278.49
10	251.69	255.06	277.14	277.78	287.23	304.56	279.81	277.85	226.29	249.76	269.70	276.73	251.69	255.06	277.14	277.78	287.23	304.56	279.81	277.85	226.29	249.76	269.70	276.73
11	235.29	250.49	272.86	276.89	271.64	292.14	279.75	279.47	227.45	228.33	270.14	270.46	235.29	250.49	272.86	276.89	271.64	292.14	279.75	279.47	227.45	228.33	270.14	270.46
12	224.57	229.96	269.03	271.06	253.29	273.52	277.45	279.85	221.17	208.49	267.64	261.74	224.57	229.96	269.03	271.06	253.29	273.52	277.45	279.85	221.17	208.49	267.64	261.74
13	254.76	283.06	279.90	279.97	308.65	336.08	277.07	268.77	214.73	262.38	275.79	278.89	254.76	283.06	279.90	279.97	308.65	336.08	277.07	268.77	214.73	262.38	275.79	278.89
14	233.02	275.05	278.97	279.91	294.84	314.39	279.21	275.78	223.89	243.87	272.76	275.34	233.02	275.05	278.97	279.91	294.84	314.39	279.21	275.78	223.89	243.87	272.76	275.34
15	240.62	260.66	274.46	278.66	279.77	297.44	280.00	278.91	220.01	228.71	267.15	270.60	240.62	260.66	274.46	278.66	279.77	297.44	280.00	278.91	220.01	228.71	267.15	270.60
16	234.81	250.77	272.71	276.95	269.15	284.62	279.58	279.92	220.57	215.38	265.09	265.09	234.81	250.77	272.71	276.95	269.15	284.62	279.58	279.92	220.57	215.38	265.09	265.09
17	247.56	269.32	278.20	279.59	296.18	301.11	279.06	278.41	212.68	243.70	270.82	275.29	247.56	269.32	278.20	279.59	296.18	301.11	279.06	278.41	212.68	243.70	270.82	275.29
18	233.83	261.66	272.39	278.80	270.80	282.58	279.70	279.98	195.92	221.40	265.75	267.74	233.83	261.66	272.39	278.80	270.80	282.58	279.70	279.98	195.92	221.40	265.75	267.74
19	237.86	360.46	273.66	256.88	272.82	275.33	279.82	279.92	207.01	207.32	260.97	261.13	237.86	360.46	273.66	256.88	272.82	275.33	279.82	279.92	207.01	207.32	260.97	261.13
Mean±SD	234.28±19.09	257.88±32.36	272.83±7.30	274.71±6.35	275.51±23.78	297.46±24.48	278.01±2.75	276.88±4.42	218.90±8.70	240.71±22.52	270.94±4.55	272.77±6.18	234.28±19.09	257.88±32.36	272.83±7.30	274.71±6.35	275.51±23.78	297.46±24.48	278.01±2.75	276.88±4.42	218.90±8.70	240.71±22.52	270.94±4.55	272.77±6.18
P	0.0095*		0.4020		0.0081*		0.3493		0.0004*		0.3049		0.0095*		0.4020		0.0081*		0.3493		0.0004*		0.3049	

\*P<0.05 was considered significant. Rt. T1: Right-side T1 value, Lt. T1: Left-side T1 value, CT1: Corrected T1 value, SD: Standard deviation

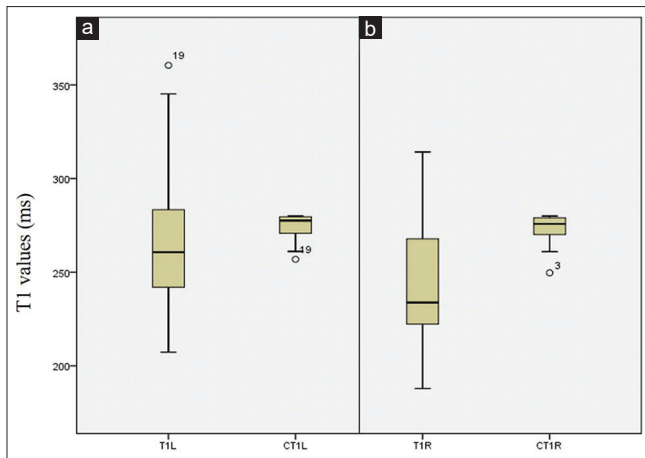


**Figure 2:** Box plot of mean T1 values. (a) T1 L and CT1 L-noncorrected and corrected T1 value distribution of the left-side breast coil. (b) T1R and CT1R-noncorrected and corrected T1 value distribution of the right-side breast coil

B1 inhomogeneity at 1.5 T was once considered negligible and B1 correction has not been a recommended feature in routine practices.<sup>[13]</sup> However, further work by Tsai *et al.* (2017) suggested the B1 inhomogeneity in VFA measurement can lead to substantial deviation (around 52%) in the T1 value of fat.<sup>[16]</sup> In the event of tumors, a 1% increase in T1 could result in a 1% decrease in  $K^{\text{trans}}$  because the measured  $K^{\text{trans}}$  value is very sensitive to the T1 value and in favor of B1 correction even at 1.5 T for more accurate T1 values for quantitative MR imaging. Quantitative DCE MR imaging at 3T is a challenge due to nonuniformity of the radiofrequency transmit field (B1+) observed across the breast coils.<sup>[15,22]</sup> Kuhl *et al.* reported a right-left signal intensity difference in breast lesions by a factor of two at 3 T due to B1 inhomogeneity.<sup>[23]</sup> This effect has also been reported at 1.5 T, although to a lesser extent.<sup>[24]</sup> Hence, B1 inhomogeneity correction has been a field of research to bring forth required accuracy in the measurement of native T1.

Several methods have been proposed to reduce the B1 nonuniformity effect on native T1 estimation. These methods include specially designed volume coils and the use of B1+-insensitive adiabatic pulses.<sup>[25,26]</sup> The B1 inhomogeneity correction exhibited a substantial effect on the quantitative estimation of PK parameters of the tumor.<sup>[17]</sup>

Pineda *et al.* used VFA and multi-inversion recovery method with reference tissue method and showed accurate B1 map in phantom data.<sup>[18]</sup> The PK modeling techniques were used to calculate native T1 of the phantom at voxel-based spatial positions. Before correction, the average absolute difference between VFA and IR values was  $58\% \pm 21\%$  ( $P < 0.05$ ); that reduced to  $8.1\% \pm 7.8\%$  ( $P > 0.05$ ) postcorrection. In the voxels with the top 10% of differences, the average values estimated to be  $170\% \pm 53\%$  without B1 correction that significantly decreased to  $28\% \pm 13\%$  after correction.

Attempts have been made to normalize measured T1 value by applying correction factor using external standards.<sup>[10,20]</sup>

However, the adopted method has inherent limitations for global homogeneity correction (bilateral breast coil cuff) with the help of a single phantom. Moreover, our study also witnessed different correction factors for each spatial location across the coil cuffs. We, therefore, tried to correct the physical space of the breast coil cuffs by applying a number of correction factors derived for each spatial location using a multiple-tube phantom placed in each coil cuff as external standards. The current approach primarily attempts to normalize the calculated T1 value from signal intensity-generated DFA images that otherwise would have been influenced by various factors such as B1 field, RF coil uniformity/sensitivity.

The circular tube phantom and the format of arrangement of the tubes adopted in this study were found to be best fitted into the breast coil cuffs. Phantom design like honeycomb pattern or methods like nearest-neighbor interpolation for correction of remaining blank spaces between each tube may further improve the extent of spatial correction of coil cuffs.<sup>[27,28]</sup>

By adopting the multiple-tube phantom-based spatial T1 estimation, we observed inhomogeneity in T1 distribution in each breast coil cuff.  $T1_0$  values in the left breast coil cuff were higher compared to the right breast cuff with the average mean difference estimated to be 22.46 ms between both sides, which postcorrection decreased to 0.86 ms. Similar observation was reported by Tsai *et al.* at 1.5 T MR imaging using B1 field correction.<sup>[16]</sup>

The current study shows significant inhomogeneity that exists across breast coil cuffs observed in the phantom study. Multiple-tube phantoms are able to provide extrinsic correction factor for spatial locations across the breast coil that achieve greater homogeneity of T1 distribution. The results derived using multi-tube phantom study for global homogenization of native T1 across breast coil cuffs are encouraging and need validation on human studies for clinical application.

### Acknowledgment

We thank Department of Physics, Vivekananda Global University, Jaipur, Rajasthan allowing to carry out this research work as part of the Ph.D. thesis program.

### Financial support and sponsorship

Nil.

### Conflicts of interest

There are no conflicts of interest.

### REFERENCES

1. Parkin DM, Bray F, Ferlay J, Pisani P. Global cancer statistics, 2002. *CA Cancer J Clin* 2005;55:74-108.
2. Kriege M, Brekelmans CT, Boetes C, Besnard PE, Zonderland HM, Obdeijn IM, *et al.* Efficacy of MRI and mammography for breast-cancer screening in women with a familial or genetic predisposition. *N Engl J Med* 2004;351:427-37.
3. Kuhl CK, Mielcareck P, Klaschik S, Leutner C, Wardelmann E, Giesecke J, *et al.* Dynamic breast MR imaging: Are signal intensity time course data useful for differential diagnosis of enhancing lesions? *Radiology* 1999;211:101-10.

4. Gilles R, Guinebretiere JM, Lucidarme O, Cluzel P, Janaud G, Finet JF, *et al.* Non palpable breast tumors: Diagnosis with contrast-enhanced subtraction dynamic MR imaging. *Radiology* 1994;191:625-31.
5. Hulka CA, Smith BL, Sgroi DC, Tan L, Edmister WB, Semple JP, *et al.* Benign and malignant breast lesions: Differentiation with echo-planar MR imaging. *Radiology* 1995;197:33-8.
6. Kelcz F, Santyr GE, Cron GO, Mongin SJ. Application of a quantitative model to differentiate benign from malignant breast lesions detected by dynamic, gadolinium-enhanced MRI. *J Magn Reson Imaging* 1996;6:743-52.
7. Perman WH, Heiberg EM, Grunz J, Herrmann VM, Janney CG. A fast 3D-imaging technique for performing dynamic Gd-enhanced MRI of breast lesions. *Magn Reson Imaging* 1994;12:545-51.
8. Fischer U, Kopka L, Brinck U, Korabiowska M, Schauer A, Grabbe E. Prognostic value of contrast-enhanced MR mammography in patients with breast cancer. *Eur Radiol* 1997;7:1002-5.
9. Veltman J, Stoutjesdijk M, Mann R, Huisman HJ, Barentsz JO, Blickman JG, *et al.* Contrast-enhanced magnetic resonance imaging of the breast: The value of pharmacokinetic parameters derived from fast dynamic imaging during initial enhancement in classifying lesions. *Eur Radiol* 2008;18:1123-33.
10. Jena A, Taneja S, Mehta BS. Role of quantitative pharmacokinetic parameters (transfer constant: Ktrans) in characterization of breast lesion on MRI. *Indian J Radiol Imaging* 2013;23:19-25.
11. Yuan J, Chow SK, Yeung DK, Ahuja AT, King AD. Quantitative evaluation of dual-flip-angle T1 mapping on DCE-MRI kinetic parameter estimation in head and neck. *Quant Imaging Med Surg* 2012;2:245-53.
12. Jena A, Taneja S, Singh A, Negi P, Mehta SB, Ahuja A, *et al.* Association of pharmacokinetic and metabolic parameters derived using simultaneous PET/MRI: Initial findings and impact on response evaluation in breast cancer. *Eur J Radiol* 2017;92:30-6.
13. Sung K, Daniel BL, Hargreaves BA. Transmit B1+ field inhomogeneity and T1 estimation errors in breast DCE-MRI at 3T. *J Magn Reson Imaging* 2013;38:454-9.
14. Azlan CA, Di Giovanni P, Ahearn TS, Semple SI, Gilbert FJ, Redpath TW. B1 transmission-field inhomogeneity and enhancement ratio errors in dynamic contrast-enhanced MRI (DCE-MRI) of the breast at 3T. *J Magn Reson Imaging* 2010;31:234-9.
15. Tofts PS, Berkowitz B, Schnall MD. Quantitative analysis of dynamic Gd-DTPA enhancement in breast tumors using a permeability model. *Magn Reson Med* 1995;33:564-8.
16. Tsai WC, Kao KJ, Chang KM, Hung CF, Yang Q, Lin CE, *et al.* B1 field correction of T1 estimation should be considered for breast dynamic contrast-enhanced MR imaging even at 1.5 T. *Radiology* 2017;282:55-62.
17. Bedair R, Graves MJ, Patterson AJ, McLean MA, Manavaki R, Wallace T, *et al.* Effect of radiofrequency transmit field correction on quantitative dynamic contrast-enhanced MR imaging of the breast at 3.0 T. *Radiology* 2016;279:368-77.
18. Pineda FD, Medved M, Fan X, Karczmar GS. B1 and T1 mapping of the breast with a reference tissue method. *Magn Reson Med* 2016;75:1565-73.
19. van Schie JJ, Lavini C, van Vliet LJ, Vos FM. Feasibility of a fast method for B1-inhomogeneity correction for FSPGR sequences. *Magn Reson Imaging* 2015;33:312-8.
20. Jena A, Mehta SB, Taneja S. Optimizing MRI scan time in the computation of pharmacokinetic parameters (Ktrans) in breast cancer diagnosis. *J Magn Reson Imaging* 2013;38:573-9.
21. Brookes AJ, Redpath TW, Gilbert FJ, Murray AD, Staff RT. Accuracy of T1 measurement in dynamic contrast-enhanced breast MRI using two- and three-dimensional variable flip angle fast low-angle shot. *JMRI* 1999;9:163-71.
22. Rahbar H, Partridge SC, DeMartini WB, Thursten B, Lehman CD. Clinical and technical considerations for high quality breast MRI at 3 Tesla. *J Magn Reson Imaging* 2013;37:778-90.
23. Kuhl CK, Kooijman H, Gieseke J, Schild HH. Effect of B1 inhomogeneity on breast MR imaging at 3.0 T. *Radiology* 2007;244:929-30.
24. Khouli El RH, Thomasson D, Pang Y, Bluemke DA. Effect of B1 Inhomogeneity Correction on T1-uniformity in Breast MRI at 1.5 Tesla: Preliminary Results. In: Proceedings of the 17<sup>th</sup> ed. Annual Meeting of ISMRM. Berkeley, California; 2009.
25. Hancu I, Lee SK, Dixon WT, Sacolick L, Becerra R, Zhang Z, *et al.* Field shaping arrays: A means to address shading in high field breast MRI. *J Magn Reson Imaging* 2012;36:865-72.
26. Staewen RS, Johnson AJ, Ross BD, Parrish T, Merkle H, Garwood M. 3-D FLASH imaging using a single surface coil and a new adiabatic pulse, BIR-4. *Invest Radiol* 1990;25:559-67.
27. Rukundo O, Cao H. Nearest neighbor value interpolation. *Int J Adv Comput Sci Appl* 2012;3:4.
28. Zhang QC, Yang X, Li P, Huang G, Feng S, Shen C, *et al.* Bioinspired engineering of honeycomb structure – Using nature to inspire human innovation. *Prog Mater Sci* 2015;74:332-400.